Title
Total Stress Analysis of Soft Clay Ground Response in Centrifuge Models

Journal
Journal of Geotechnical and Geoenvironmental Engineering, 145(10)

ISSN
1090-0241

Authors
Afacan, Kamil B
Yniesta, Samuel
Shafiee, Ali
et al.

Publication Date
2019-10-01

DOI
10.1061/(asce)gt.1943-5606.0002115

Peer reviewed

Total Stress Analysis of Soft Clay Ground Response in Centrifuge Models

by: Kamil B. Afacan[1], Samuel Yniesta[2], Ali Shafiee[3], M. ASCE, Jonathan P. Stewart[4], F. ASCE, and Scott J. Brandenberg[5], M. ASCE.

Abstract: This paper presents one-dimensional ground response simulations of centrifuge models involving soft clay deposits subjected to ground motions of varying intensity. Total stress ground response simulations were performed using equivalent-linear (EL) and nonlinear (NL) methods. Shear strains higher than 10% were mobilized during large ground motions, therefore undrained shear strength of the clay is an important parameter for the simulations. Testing shows that the Bay Mud materials used in centrifuge modeling have monotonic shear strengths that increase by 13% per log cycle of shear strain rate. Comparison of simulation results to observations reveals the importance of incorporating shear strength into the development of stress-strain backbone curves, with appropriate consideration of rate-adjustments to shear strength and stiffness. NL ground response simulations provide a good match to observed pseudo-spectral accelerations only when rate-adjusted shear strengths are properly accounted for, otherwise the NL simulations have significant under-prediction bias at oscillator periods less

[1] Assistant Professor and Vice Chair, Dept. Civil Engineering, Eskisehir Osmangazi University, Eskisehir/Turkey.
[2] Assistant Professor, Dept. Civil, Geological and Mining Engineering, Polytechnique Montréal, Montréal QC, Canada
[3] Assistant Professor, California State Polytechnic University, Pomona, CA, 91768
[4] Professor, Dept. Civil & Environmental Engineering, University of California, Los Angeles, 90095
[5] Professor, Dept. Civil & Environmental Engineering, University of California, Los Angeles, 90095, email: sjbrandenberg@ucla.edu; Corresponding Author.

than the soil column period. EL modeling, even with incorporation of shear strength, leads to unrealistic spectral shapes and over-prediction at short spectral periods for tests involving large-strain site response.

INTRODUCTION

Earthquake ground motions are influenced by source, path and site effects. Site effects, the topic of this paper, are commonly approximated in contemporary codes, standards, and ground motion models using ergodic (i.e., not site-specific) nonlinear site amplification functions, which are often conditioned on the time-averaged shear-wave velocity in the upper 30 m of the site (V_{S30}) (e.g., Borcherdt, 1994; Dobry et al. 2000). Site amplification functions are typically developed using statistical analysis of measured ground motions, and may be constrained by ground response simulations for conditions poorly represented in empirical databases. Because ergodic models are not site specific, in effect they capture the average site response observed across many regions, conditional on a particular value of the independent variable used in the model (V_{S30} and perhaps others). Non-ergodic (site-specific) analyses of site response can better account for site-specific conditions and can be coupled with an aleatory variability model for ground motions that removes the site-to-site component of variability. Due to this reduction of aleatory variability, probabilistic seismic hazard analyses using a non-ergodic site function will often provide lower hazard estimates for long return periods than would be provided with an ergodic model (Stewart et al., 2017).

Site-specific analyses of site effects are most typically performed using one-dimensional (1D) ground response analysis (GRA) procedures employing either equivalent-linear (EL) or nonlinear (NL) methods (e.g., Matasovic and Hashash 2012). One-dimensional GRA is limited to vertically propagating shear waves, and does not capture the influence of inclined body waves and surface waves on ground surface motion; consideration of such conditions is beyond the scope of the present manuscript (see, for example, Stewart et al. 2014 for more information).

Many of the practical applications that motivate site-specific ground response analyses involve soft soils and strong input ground motions, for which highly nonlinear responses will occur. For such conditions, predictions from NL and EL methods have been shown to differ substantially, especially at high frequencies (e.g., Kim and Hashash, 2013; Kaklamanos et al., 2013, 2015; Zalachoris and Rathje, 2015; Kim et al., 2016). A remaining challenge, however, is the validation of ground response estimates (whether NL or EL) against data for highly nonlinear conditions. While some downhole arrays have recorded nonlinear responses, those responses have generally not been so severe as to approach the shear strength of the soil within portions of the profile. It is this condition, commonly encountered in design applications involving soft soil sites, that Afacan et al. (2014) investigated using centrifuge models of soft, lightly over-consolidated clay deposits. The objective of the present manuscript is to perform validation exercises for EL and NL ground response analysis programs using the Afacan et al. (2014) data set. Simulations are performed in a total stress framework since pore pressure development in the models was not significant (excess pore pressure ratios after shaking were less than 0.1, and often essentially zero). Pore pressure development and liquefaction are also important nonlinear site response considerations, but are beyond the scope of this paper.

Following this introduction, we describe aspects of the centrifuge models that are most directly pertinent to ground response analysis (details in Afacan et al., 2014). The influence of strain rate on the undrained shear strength and stiffness of the clay used in the centrifuge modeling is then presented, along with a review of techniques used to model shear strength in various nonlinear ground response analysis platforms. Ground response simulations are then compared with experimental data to investigate the following modeling aspects: (1) consideration of undrained shear strength and rate effects, (2) different NL modeling platforms [DEEPSOIL (Hashash et al., 2016) versus OpenSees (Mazzoni et al. 2009)], and (3) different modeling approaches (NL versus EL).

CENTRIFUGE MODELS

An experimental program using the UC Davis 9m radius geotechnical centrifuge was performed to study the nonlinear site response behavior of soft clay deposits (Afacan et al. 2014). The model configuration consisted of reconstituted, lightly overconsolidated San Francisco Bay Mud (plasticity index PI = 40, virgin compression index C_c = 0.43, recompression index C_r = 0.04) overlying more heavily overconsolidated Bay Mud (Fig. 1). A layer of coarse dense sand was placed atop the lightly overconsolidated Bay Mud, and lifts of clay were separated by coarse dense sand to provide drainage during consolidation of the clay from slurry and during centrifuge spinning. A hinged-plate container that is very flexible and light was used in this study to accurately produce 1-D site response boundary conditions. The effectiveness of the hinged-plate container was documented by Afacan et al. (2014). Figure 1 shows profiles of vertical effective stress, preconsolidation stress, shear wave velocity, and monotonic undrained shear strength.

The undrained strength profile is shown to be rate-dependent later in this paper. The monotonic undrained shear strength profile was computed as:

$$s_{uc} = 0.22 \cdot \sigma_v' \cdot OCR^{0.8} \qquad (1)$$

where s_{uc} is monotonic undrained shear strength, σ_v' is vertical effective stress, OCR is overconsolidation ratio, and the coefficient 0.22 was derived from simple shear testing of reconstituted Bay Mud materials prepared in the same manner as the clay deposits in the centrifuge models. The coefficient 0.8 was assumed (Ladd, 1991). Note that the coefficient has little influence on the strength of the shallower layers that are essentially normally consolidated. We anticipate that the ground response analyses are significantly influenced by the response of the shallower layers, and are therefore relatively insensitive to selection of the coefficient. The rate-dependence of Bay Mud strength is presented subsequently.

The sequence of imposed ground motions ranged from very low-amplitude, inducing essentially elastic soil response, to very high amplitude, generating shear strains in excess of 10% in some layers. Motions recorded in the clay near the base of the model container were utilized as input motions for the ground response simulations. Motions recorded at the base plate of the model container were not utilized due to slip between the base plate and the thin latex membrane liner placed between the soil and the hinged plate container. Peak accelerations in the clay near the base of the models ranged from 0.02g to 0.6g.

INFLUENCE OF STRAIN RATE ON SOIL RESPONSE

The dynamic response of soil is known to depend on strain rate ($\dot{\gamma}$). For example, Sheahan et al. (1996) found that the peak shear strength of normally consolidated and lightly overconsolidated Boston blue clay increased approximately 5 to 12% per log cycle of strain rate for $\dot{\gamma}$<10^{-5}%/s to 0.01%/s. Lefebvre and LeBoeuf (1987) investigated four Canadian clays under normally and overconsolidated conditions and found a 7 to 14% increase in undrained strength per log cycle of strain rate for a $\dot{\gamma}$ range of 10^{-5}%/s to 1%/s. Fully softened and residual strengths have also been shown to increase at rapid (vs slow) loading rates in ring shear and sliding block studies (Khosravi et al., 2013; Meehan et al., 2008). Given this prior work, two knowledge gaps are especially pertinent for this study: (1) rate effects on undrained strength have been investigated for relatively few soil materials, and the applicability of the prior results for Bay Mud are unknown, and (2) the trend in strength increase with rate of cyclic loading has not been adequately investigated at strain rates higher than 1%/s, which are believed to be important for highly nonlinear soil response during seismic loading. Cohesionless soils also exhibit strain rate effects, albeit to a lesser extent than clays (e.g., Matesic and Vucetic 2003).

Strain rate also influences secant stiffness, and is therefore a factor that must be considered at all strain levels. Isenhower and Stokoe (1981) found that secant shear modulus of Bay Mud increases with strain rate for $\dot{\gamma}$>10^{-6}%/s to 0.1%/s, and that the increase per log cycle is essentially independent of the strain amplitude. The latter observation implies that the normalized modulus reduction curve is independent of strain rate. Matesic and Vucetic (2003) performed cyclic direct simple shear test at small strains on sand and clay samples, and confirmed that the normalized modulus reduction curve is independent of shear strain rate at strains lower than 0.01%, for $\dot{\gamma}<10^{-4}$%/s to 0.01%/s.

The critical issue for seismic ground response problems is whether observed rate effects measured at slow rates in typical laboratory test devices can be extrapolated to much faster rates that may occur during an earthquake. The recommendations of Sheahan et al. (1996), which are similar to those of Lefebvre and LeBoeuf (1987), have been assumed to apply at faster rates in some previous applications (e.g., Boulanger and Idriss, 2007) and in seismic analysis guidelines (Blake et al., 2002). Yong and Japp (1964) present a contradictory finding whereby notably larger strength increases were found when $\dot{\gamma}$ > 100%/s, suggesting that rate corrections developed at slower rates may not always extrapolate well to faster rates. While important for ordinary site response problems, these strain rate corrections are particularly important for centrifuge modeling because strain rate scales with g-level and hence is much higher at model scale than prototype.

A sequence of simple shear tests was performed using the digitally controlled direct simple shear device at UCLA (Duku et al. 2007; Shafiee et al. 2017) to investigate the influence of strain rate on the undrained shear strength of the Bay Mud used in centrifuge modelling. Monotonic constant height strain-controlled loading was imposed on reconstituted specimens at strain rates of 0.01%/s, 0.1%/s, 1%/s, and 10%/s. The specimens were consolidated from slurry in a tube to a vertical effective stress of about 10 kPa, trimmed into a wire reinforced latex membrane, and subsequently consolidated in the simple shear device to a vertical effective stress of 50 kPa. The shear stages were repeated without a specimen to ascertain the influence of device inertia on measured loads, and the inertial loads were subtracted from the soil response (inertia forces were essentially negligible for all but the fastest strain rate). An overconsolidation ratio of 1.15 was targeted for testing, but slightly higher OCR's ranging from 1.20 to 1.31 were achieved due to stress relaxation between the time the simple shear device was placed in vertical displacement control to achieve constant volume conditions and the time shearing commenced. For a uniform comparison among specimens with slightly variable OCR's, the normally-consolidated strength ratio was computed as $(s_u/\sigma_{vc}')_{NC} = (s_u/\sigma_{vc}')/OCR^{0.8}$ (the exponent of 0.8 is taken from Ladd, 1991). Shear strength was interpreted as the horizontal plane shear stress (τ_{HV}) mobilized at 10% shear strain. This definition of shear strength was selected because it is close to the limit of the direct simple shear device, and because it is consistent with the definition of shear strength adopted later when computing shear strength implied by extrapolating modulus reduction equations to large strain. Shear strength is plotted as a function of strain rate in Fig. 2.

The laboratory measurements were regressed using Eq. 2 to solve for factors ρ_{γ} and γ_{ref}, which represent the average change of undrained strength per log cycle of $\dot{\gamma}$, and the strain rate associated with a normally consolidated undrained strength ratio of 0.22, respectively:

$$\left(\frac{s_u}{\sigma_{vc}{}'}\right) = 0.22 \cdot OCR^{0.8} \cdot {\rho_\gamma}^{log\left(\frac{\dot{\gamma}}{\dot{\gamma}_{ref}}\right)} \qquad (2)$$

The regression indicates that $\dot{\gamma}_{ref}$=0.08%/s, and ρ_γ = 1.13, which can be compared to the approximate range of ρ_γ = 1.05-1.12 from Sheahan et al. (1996) and 1.07 to 1.14 from Lefebvre and LeBoeuf (1987). The value of $\dot{\gamma}_{ref}$ is higher than a typical laboratory strain rate of about 0.0014%/s (5%/hour). Substituting $\dot{\gamma}$=0.0014%/s and OCR = 1.0 into Eq. 2 results in $\left(\frac{s_u}{\sigma_{vc}{}'}\right)$=0.18, which is on the low end of normally consolidated strength ratios for undisturbed San Francisco Bay Mud. It is likely that the lower normalized strengths obtained in this study result at least in part from the use of reconstituted specimens.

In addition to the laboratory test data, Fig. 2 also shows shear stresses mobilized during centrifuge tests for cycles where shear strains exceeded 10%, with correction to an equivalent normally consolidated condition by dividing the mobilized stresses by $OCR^{0.8}$. The curve fit to the laboratory data lies slightly above the centrifuge data points with peak mobilized cyclic shear strains, γ_c, equal to 10% and 11%, and slightly below the data point with γ_c=21%. The consistency of these data with the simple shear trend indicate that rate effects observed at slow rates in the laboratory do in fact extrapolate well to high rates. This indicates that ρ_γ is constant, and does not increase suddenly at high strain rate, as implied by the results of Yong and Japp (1964). Further, it suggests that Eq. 2 provides an appropriate strain rate correction for analysis of the centrifuge tests.

Centrifuge scaling laws result in model scale strain rates that are higher than those anticipated at an equivalent prototype site by an amount equal to the centrifugal acceleration (e.g., Garnier et al. 2007), but the strength correction would nevertheless be important at the prototype scale. The peak strain rate mobilized in the centrifuge experiments (conducted at 57g) was about 6600%/s, which is associated with $(s_U/\sigma_{vc}')_{NC}$=0.40 based on Eq. 1. The equivalent prototype strain rate is (6600%/s)/57 ≈ 100 %/s resulting in a still significant rate effect corresponding to $(s_U/\sigma_{vc}')_{NC}$=0.32. Accordingly, the importance of the strain rate correction is not merely an artifact of centrifuge modeling, and is important to consider for practical problems involving earthquake shaking of soft soils.

CORRECTION OF MODULUS REDUCTION CURVE TO OBTAIN DESIRED SHEAR STRENGTH

Modulus reduction curves are commonly computed using empirical models employing a hyperbolic function in which model parameters are derived from cyclic laboratory tests that extend to strain amplitudes as high as about 0.3% (e.g., Darendeli 2001). Many combinations of earthquake ground motions and soil conditions will result in peak strains that are lower than 0.3%, in which case analyses can be performed within the range of experimental validation of these modulus reduction curves. However, strong ground motions imposed at the base of soft soil layers may result in shear strains that exceed 0.3%, possibly mobilizing shear failure in extreme conditions, as occurred in the centrifuge models. This is precisely the scenario for which NL ground response analyses are anticipated to provide the largest benefit relative to EL. This section illustrates the error in the shear strength that is implied by simply extrapolating a modulus reduction equation to high strain. We then discuss a procedure developed by Yee et al. (2013) and adopted in subsequent sections of the paper, to correct the large-strain tail of a modulus reduction curve to provide a desired strength, and compare it with several recent constitutive models that are capable of matching a target strength.

The hyperbolic model, which is commonly used to model modulus reduction curves, is typically written as (Darendeli, 2001):

$$\frac{G}{G_{max}} = \frac{1}{1 + \left(\frac{\gamma}{\gamma_r}\right)^a} \tag{3}$$

where a is a shape parameter and γ_r is referred to as the pseudo-reference strain, which is given as (Darendeli, 2001):

$$\gamma_r = \left(\phi_1 + \phi_2 \cdot PI \cdot OCR^{\phi_3}\right)\left(\frac{p'}{p_a}\right)^{\phi_4} \tag{4}$$

The ϕ_i coefficients are empirically derived, $p'=\sigma_v' \cdot (1+2 \cdot K_o)/3$, $K_o=(1-\sin \phi') \cdot OCR^{\sin\phi}$ (Mayne and Kulhawy, 1982), ϕ'= effective friction angle (taken as 26° based on the simple shear test results with the lowest strain rate, deemed most appropriate for computing K_o), and p_a is atmospheric pressure. Values of the empirical constants computed by Darendeli (2001) for clays from northern California are a=0.919 ϕ_1=0.0339, ϕ_2=0.00175, ϕ_3=0297, and ϕ_4=0.278. These coefficients were based on tests performed on native soils, whereas the Bay Mud tested in the centrifuge was reconstituted from slurry. Nevertheless, these region-specific coefficients are believed to be representative of reconstituted Bay Mud. The value of G_{max} was obtained from the V_s profile in Fig. 1.

A stress-strain curve can be computed from a modulus reduction curve as $\tau = G_{max} \cdot (G/G_{max}) \cdot \gamma$. A true shear strength, defined as a peak or horizontal asymptote for the hyperbolic stress-strain curve, does not exist for a<1.0. Therefore, an implied shear strength is taken as the shear stress at 10% shear strain. Values of implied shear strength were computed for the soil profile in Fig. 1, and are plotted vs. depth in Figure 3 along with the monotonic undrained shear strengths $[(s_u/\sigma_{vc}')_{NC} = 0.22]$ and the rate-corrected shear strengths $[(s_u/\sigma_{vc}')_{NC} = 0.40]$. The implied shear strengths produced by extrapolation of the hyperbolic equation are significantly lower than the monotonic and rate-corrected undrained shear strengths in this case. This clearly illustrates that the hyperbolic equations should not simply be extrapolated to large strain, but rather procedures must be adopted to provide the desired shear strength (whether selected as-measured or rate-corrected). Furthermore, the rate correction is significant in this case.

The method adopted in this paper by Yee et al. (2013) modifies the large-strain portion of a modulus reduction curve to achieve a desired shear strength. Beyond a transition strain (γ_t) the stress-strain curve is defined using a hyperbolic function that asymptotically approaches the desired shear strength, while maintaining a continuous slope in the stress-strain curve at the transition strain. Below the transition strain, hyperbolic models as in Eq. (3) are used. Yee et al. (2013) recommend selecting the largest possible value of γ_t to preserve the desired small-strain nonlinearity, while ensuring that the shear stress at γ_t is less than about 1/2 to 1/3 of s_u so that the hybrid procedure produces a smooth transition to s_u at large strains.

The procedure is demonstrated for soil located at the center of the upper lift of clay from centrifuge experiment AHA02 (Afacan et al. 2014) for which PI = 40, OCR = 1.29, V_s = 83 m/s, ρ = 1.6 Mg/m^3, σ_v' = 65 kPa, monotonic s_{uc} = 17 kPa, and rate-corrected s_u = 32 kPa. Secant shear modulus (G) and stress (τ) vs. strain using the extrapolated hyperbolic model from Eq. (3) are plotted in Fig. 4 along with the hybrid procedure with γ_t=0.1% for both the monotonic and rate-corrected values of s_u. As in Fig. 3, the implied strength from extrapolation of the hyperbolic curve to high strain results in a shear strength that is significantly less than the monotonic and rate-corrected undrained shear strengths. Fig. 4 shows that the hybrid procedure produces seemingly small differences in the modulus reduction curve at large strains but large differences in shear strength. Note that the as measured and rate corrected modulus reduction curves are the same because the same rate correction is applied to both s_u and G_{max}.

The Yee et al. (2013) procedure is one approach that renders a modulus reduction curve that matches a desired strength, but there are other options that also solve this problem. The GQ/H model recently implemented in DEEPSOIL by Groholski et al. (2016) uses a quadratic equation to fit the modulus reduction curve at strains lower than a specified shear strain level, and to match a target shear strength at large strains. The PressureDependMultiYield (PDMY) and PressureIndependMultiYield (PIMY) material models implemented in OpenSees by Elgamal et al. (2003) utilizes a set of nested yield surfaces to control plastic modulus. The nested yield surfaces and associated plastic modulus values can be adjusted to match a user-specified modulus reduction curve. The largest yield surface is set to provide the desired shear strength. The Yee et al. (2013) procedure could be utilized to produce the user-specified modulus reduction curve. Yniesta and Brandenberg (2017) suggested that G/G_{max} could be plotted versus stress ratio (q/p' or τ/σ_v') rather than shear strain. Using this procedure, the strength is controlled by the highest stress ratio specified in the modulus reduction formulation rather than by large-strain tail of the modulus reduction curve.

MATCHING SPECIFIED MODULUS REDUCTION AND DAMPING CURVES

A user-specified modulus reduction curve may differ from the hyperbolic functional form in Eq. 3, as well as other functional forms adopted in various modeling platforms. Formulations for fitting or matching a specified modulus reduction curve by Groholski et al. (2016), Yniesta et al. (2017), and Elgamal et al. (2003) are discussed here. All three of these approaches are capable of matching a desired shear strength, and we focus our attention here on the remaining portion of the modulus reduction curve.

Figure 5 presents the predictions of the three models for the target modulus reduction and damping curves at a depth of 6.5m, which is where the maximum shear strain occurred during centrifuge testing. The GQ/H model uses a regression procedure to fit the functional form of the backbone curve to the specified modulus reduction curve, and therefore generally involves a slight misfit of the curve but a good match of the target shear strength. The ARCS model (Yniesta et al. 2017), implemented as a user-defined material model in DEEPSOIL, fits the specified modulus reduction data points with cubic spline interpolation functions and therefore exactly matches the modulus reduction curve at the specified ordinates. The PIMY and PDMY material models also match the desired modulus reduction curve, though the stress-strain behavior is piecewise linear, whereas the GQ/H and ARCS models produce smoothly varying stress-strain curves.

Implementation of hysteretic damping and small-strain damping is also model-specific. Hysteretic damping is controlled by the unload-reload rule. The target damping curves used in this study were those by Darendeli (2001). In DEEPSOIL, the GQ/H model is used in conjunction with the MRDF-UIUC unload/reload rule (Phillips and Hashash 2009) to match a target hysteretic damping curve. This procedure generally results in a small misfit between the specified damping curve and the one achieved by the model. The ARCS model uses a coordinate transformation rule to control the damping behavior (Yniesta et al. 2017), providing an exact match to the user-specified damping curve. The PDMY and PIMY models utilize Masing's rules, which provide damping that is too high at large strains. Kwok et al. (2007) discussed various methods for matching the modulus reduction and damping curves using codes that rely upon Masing's rules.

In this paper, we match the modulus reduction curve, and accept a misfit in hysteretic damping using OpenSees.

Small-strain damping is inherently included in the hysteretic damping formulation in the ARCS model. Users specify the desired damping level at small strain, and the hysteretic formulation provides the specified level of damping. However, small-strain damping is not captured hysteretic formulations in either DEEPSOIL or OpenSees, and must be independently introduced to the system of equations. Small-strain damping in DEEPSOIL is modeled using a frequency-independent Rayleigh damping formulation developed by Phillips and Hashash (2009). This implementation is not available in OpenSees, so full Rayleigh damping (i.e., in which damping is specified at two frequencies) is utilized instead. Selected matching frequencies were 0.3Hz and 5Hz, with lower damping between these two frequencies and higher damping at higher and lower frequencies. These frequencies were selected to bracket the frequency content of the ground motions imposed on the models. Often, the lower frequency is set based on the first mode frequency of the soil column and the higher frequency is set to be some multiple of the first mode frequency. However, this approach is not appropriate for nonlinear problems where the first mode frequency may decrease significantly as a result of strong shaking. We therefore opted to set the Rayleigh damping frequencies to bracket the frequency content of the input ground motions. The target small strain damping level for the clay was estimated to be 8% based on measurements of the present set of centrifuge tests excited by small vibrations. Literature shows that damping in centrifuge models is often higher than values based on laboratory testing (e.g., Brennan et al. 2005). The small strain damping for the sand layers was set to 2% to account for combined effects of material damping and relative movement of the sand particles and pore water at the excitation frequencies (Qiu, 2010).

GROUND RESPONSE MODELING

Six ground response analysis modeling configurations were used to simulate the centrifuge data, as summarized in Table 1. Modeling variations include modeling platform (DEEPSOIL and OpenSees), analysis approach (NL and EL), constitutive model used (for NL approach), whether the modulus reduction curve was corrected for shear strength, and whether a rate correction was applied to strength and stiffness. The rate correction is the $\rho_\gamma^{log\left(\frac{\dot{\gamma}}{\gamma_{ref}}\right)}$ term from Eq. 2, where ρ_γ = 1.13 and $\dot{\gamma}_{ref} = 0.08\% / s$ were obtained by regression from the laboratory experiments presented previously, and $\dot{\gamma}$ =6600%/s was used for Models 3 – 6. The resulting rate correction value for shear modulus and shear strength is 1.82. Note that the shear wave velocity increases by the square root of this value (1.35), which influences site response by stiffening the profile. Therefore, the rate correction applied herein influences ground motion across a broad strain range, and not just at large strains where the shear strength is anticipated to be the dominant factor.

The profiles were discretized into 50 layers to adequately capture the frequency content of input ground motions. As described by Phillips et al. (2012), soil elements that are too tall cause spatial aliasing that results in a low-pass filter that prevents propagation of short wavelengths. Adequacy of the discretization was verified by observing similar response for simulations with more elements (Afacan 2014). The friction angle for the sand layers was set to 40°, which is reasonably consistent with estimates following Bolton (1986), assuming a critical state friction angle of 32° for the Monterey sand. Analysis results are insensitive to the sand strength.

GROUND RESPONSE MODELING RESULTS

In this section, we compare ground response simulation results to test data. Pseudo-spectral accelerations (PSAs) are presented first for a single input ground motion scaled to three different amplitudes. These analyses are intended to illustrate the influences of undrained shear strength, modeling platform (DEEPSOIL and OpenSees), and modeling approach (NL versus EL) on computed PSAs. The features of the data-simulation comparisons are then evaluated in a statistical manner using a selection of input motions through residuals analysis (residuals being defined as the difference of natural logs of measured and simulated intensity measures).

Influence of Undrained Shear Strength and Stiffness

Response spectral amplification factors and 5% damped PSA are plotted in Fig. 6 for three scaled versions of the RRS228 horizontal component of the ground motion recorded at the Rinaldi Receiving Station during the 1994 **M**6.7 Northridge earthquake. The peak recorded PGA was

0.838g. The centrifuge shake table cannot perfectly replicate a target ground motion, so the response spectra for the imposed base motions differ from the target motions, and there are slight variations in spectral shape as intensity increases. Measured surface PSAs are compared with computed results from Models 1, 2, and 3 and the base motion spectrum is included as a reference. The site period inferred from the spectral amplification factors is about 1.0, 1.5, and 2.0 seconds for the small, medium, and large amplitude motions, respectively. Models 1 and 2 consistently under-predict the surface motion for periods less than the site period, with the error increasing as shaking intensity increases. All three models predict spectra similar to those from measurements at periods longer than the site period. The predictions from Model 3, which use rate-adjusted shear strengths with the hybrid backbone curve, are in better agreement with the observations.

We expect that several factors are responsible for the differences among predictions for Models 1-3. Peak mobilized shear strains were about 0.15%, 1.5%, and 4.5% for the small, medium, and high-intensity motions, respectively, as illustrated in Fig. 7. Although all three models tend to over-predict shear strain, Model 3 provides the most accurate predictions. It is therefore no surprise that Model 3 surface motions agree most closely with measured surface motions. Models 1 and 2 tended to under-predict ground surface motion due to the following two factors: (1) the higher mobilized strains resulted in higher damping, thereby reducing ground motion, and (2) shear strains during the medium and high intensity ground motions mobilized a significant fraction of the undrained shear strength, thereby limiting the shear stresses transmitted through the layers (recall that undrained strength is lowest for Model 1, and highest for Model 3).

Comparison of simulation results across analysis platforms

Using the same Northridge input motions as in the previous section, Fig. 8 compares observed and predicted PSA, as well as spectral amplification factors, for non-linear simulations in alternate platforms utilizing hybrid backbone curves with rate-adjusted shear strengths (Models 3-5). Results of equivalent linear (EQL) simulations in DEEPSOIL (Model 6) are also shown, which are discussed in the next section. Because the backbone curves are similar, the primary difference between the analysis procedures is the hysteretic and small-strain Rayleigh damping formulations. DEEPSOIL (Models 3-4) is able to more accurately capture both sources of damping than the models implemented in OpenSees (Model 5). For this reason, we anticipated over-damping at high strain in the OpenSees model due to the Masing rule formulation. However, the influence of this overdamping appears to be modest in this case, which is likely a result of the modest thickness of the soil column.

Comparison of Nonlinear and Equivalent-Linear Simulations

Kim et al. (2016) showed that EL and NL ground response results diverge significantly when the strain index, defined as $I_r=PGV_r/V_{s30}$, exceeds about 0.03% (where PGV_r is the peak velocity of the input motion). Observed divergences of the analysis results included a long flat portion of the EL spectrum at short periods, often extending to 0.1-0.2 sec, and stronger resonant peaks in the EL spectrum near the site period. It is important to note that this prior work made judgments about when NL is preferred to EL based on divergence of simulation results, the key point being that there was no data against which to compare the simulations. The present results enable EL-NL comparisons for cases where observed responses are also available.

Fig. 8 shows observed and predicted PSA for NL (Model 3, 4 and 5) and EL (Model 6) ground response simulations. Both models utilized hybrid backbone curves with rate-adjusted shear strengths. Values of the strain index for the three input motions are I_r = 0.05, 0.15, and 0.40%, which all exceed the threshold recommended by Kim et al. (2016). For all three input motions, the EL spectrum is flatter at short periods than the NL spectrum, although the differences become much more pronounced as the strength of shaking increases. It is significant that the data produce a non-flat spectral shape in this period range, being more consistent with the NL results.

The peak in the spectral amplification function is interpreted as corresponding to the site period, which is approximately 0.8 s, 1.0 s, and 2.0 s sec for the three input motions (Fig. 8d, 8e and 8f). Distinctions between EL and NL apparent from spectra (Figs. 8a-c) include: (1) the spectral peaks at the site periods are stronger in EL compared to those from NL models; (2) EL PSAs for periods shorter than the site period are larger than NL in all three cases. PGAs are over-predicted by nearly a factor of 2 by the EL model whereas the NL models are reasonably accurate.

The EL simulations presented herein utilized rate-corrected shear strength. Although not shown here, EL simulations that utilize monotonic shear strengths (like Model 2), or fail to correct the modulus reduction curve to provide a desired shear strength (like Model 1) result in a significant under-prediction of ground motion.

PSA Residuals for All Motions

Prior sections have illustrated how simulation results compare to data, but are based on a single input motion scaled to three amplitudes. A much broader suite of testing was performed as part of the centrifuge modeling using additional input motions over a wide range of amplitudes. Model predictions are compared with measurements for this broad suite of input motions using residuals analysis. Details of these additional input motions are described by Afacan et al. (2014). Residuals are defined using ground motion intensity measures as follows:

$$R_i = \ln Y_{obs,i} - \ln Y_{sim,i} \tag{4}$$

where $Y_{obs,i}$ is the i^{th} observation of an intensity measure (i.e., from the centrifuge testing) and $Y_{sim,i}$ is the corresponding estimate from a simulation. Index *i* spans from one to 19 (where 19 = number of input motions). The intensity measures that are considered are PSAs at 5% damping for oscillator periods between 0.01 and 10 sec.

Residuals for spectral acceleration are plotted in Fig. 9 with different symbols for small-amplitude input motions (base peak acceleration, PGA_b < 0.1g, $I_r \lesssim$ 0.05%) and medium- to large-amplitude input motions (PGA_b > 0.1g, $I_r \gtrsim$ 0.05%). We also show median residuals within the respective PGA_b ranges for each period. For PGA_b < 0.1g, all the models produce similar results, with differences largely attributed to the rate correction of strength and stiffness, and resulting higher mobilized strain and hysteretic damping for the softer models. For stronger input motions, the trends of the results are summarized below:

- Model 1-2 results have large under-prediction bias (positive residuals), which is an outcome of shear strength being too low in these simulations.
- Model 3 and Model 4, using DEEPSOIL with rate-corrected shear strengths, are effectively unbiased across the considered period range for the PGA_b > 0.1g bin. There is some overprediction bias (negative residuals) for weaker motions, which may be caused by an under-prediction of damping.
- The models, to varying extents, exhibit an abrupt transition in residuals at a spectral periods around 0.8s to 1.0s for PGA_b < 0.1g, and around 1 to 3s for PGA_b > 0.1g. This abrupt change occurs at spectral periods near the site period, which is shorter for PGA_b < 0.1g and longer for PGA_b > 0.1g. Model 6, using EL with rate-corrected shear strengths, exhibits over-prediction bias at short periods and under-prediction bias at periods longer than about 1.5s. The short period overprediction bias occurs because the flat, short-period plateau has an amplitude that is high relative to observations; this likely occurs because the over-predicted site resonance is controlling the short-period oscillator responses.

CONCLUSIONS

Site-specific analyses of earthquake ground motions will often include the use of non-ergodic site terms based on 1D ground response modeling. Such analyses are recommended for soft soil sites where strong input motions can lead to significant nonlinearity, which in turn is thought to necessitate the use of NL, as opposed to EL, methods of analysis (Matasovic and Hashash, 2012; Stewart et al., 2014; Kim et al. 2016). Previous research has shown that NL and EL analyses produce different results for highly nonlinear conditions, but very little data from field downhole arrays exists to validate analysis results. This research addresses that knowledge gap by comparing 1D ground response simulation results with data from centrifuge modeling of soft clay subjected to strong base motion that induced large shear strains (> 10%), resulting in shear failure of the soil. A range of ground response simulation types were utilized to investigate sensitivity to modeling approach (NL vs EL), the manner by which shear strength is represented in the soil backbone curve, rate-correction of shear strength and stiffness, and NL modeling platform (DEEPSOIL versus OpenSees).

The undrained shear strength of the San Francisco Bay mud utilized in the centrifuge models was found to scale strongly with strain rate ($\dot{\gamma}$). Monotonic shear strength was found to increase approximately 13% per log cycle of $\dot{\gamma}$, which produces strength increases of about 80% for the centrifuge models, where peak strain rates were as high as 6600%/s. The measured strain rate influence is specific to the Bay Mud tested in this paper, and is more pronounced than for lower plasticity clays (e.g., Lefebvre and LeBoeuf 1987, Sheahan et al. 1996). Engineers are encouraged to use judgment in extrapolating these observed rate effects to other types of clay.

Utilizing strain-rate-compatible profiles of undrained shear strength and stiffness was crucial for obtaining accurate ground response predictions. Under-predictions of shear strength, either by ignoring shear strength in the development of backbone curves or failing to make appropriate rate adjustments, substantially reduced predicted pseudo-spectral acceleration (PSAs) of surface ground motions. Those reduced PSAs fall below observations, thus confirming previous findings that shear strength needs to be considered in the development of backbone curves (Yee et al., 2013; Zalachoris and Rathje 2015) and that shear strength and stiffness parameters require rate adjustment. Strength and stiffness are often assigned values lower than their median estimate in design applications based on the assumption that under-estimating these parameters is conservative. The opposite was found to be true in this study; under-estimating undrained strength and stiffness resulted in a corresponding under-estimation of ground motion. We therefore recommend that engineers utilize unbiased estimates of strength and stiffness and apply corrections for strain rate effects in their site response calculations. One point of departure between our findings and those of some others using vertical array data (Zalachoris and Rathje 2015; Kaklamanos et al. 2013), is that those previous studies found that ground response simulations under-predict surface motion when the input shaking intensity is high. It is unclear the extent to which rate effects were considered in those studies; as shown here, consideration of such effects tends to increase predicted ground motions at periods smaller than the site period.

When rate-corrected undrained shear strengths were used, EL simulations overestimated PGA by almost a factor of two, whereas NL simulations (both GQ/H and ARCS models in DEEPSOIL) were reasonably accurate. Based on these simulation-data comparisons, we concur with recommendations from previous research recommending NL modeling over EL when large strain conditions are encountered (Kim et al., 2016; Kaklamanos et al., 2013, 2015; Zalachoris and Rathje, 2015). Note that EL simulations under-predicted short period ground motions when monotonic undrained shear strengths were used.

Ground motion residuals exhibit an abrupt transition at spectral accelerations near the site period, and residuals for all of the nonlinear models at spectral periods beyond the site period were all reasonably consistent and close to zero. This is an indication that ground response analysis procedures are most appropriate for modeling ground motions shorter than the site period. Under field conditions, amplification of ground motions longer than the site period may be controlled by other factors, such as basin geometry, and velocity structure below the base of the ground response models. Caution should be used when interpreting long-period amplification from ground response analysis simulations.

Acknowledgments

We would like to thank former UCLA MS student Alek Harouonian and the NEES@UCDavis personnel, including Dan Wilson, Ross Boulanger, Bruce Kutter, Chad Justice, Ray Gerhard, Peter Rojas, Lars Pederson, Anatoliy Ganchenko, and Jenny Chen for their assistance during the centrifuge modeling. We would like to thank Youssef Hashash for his input related to DEEPSOIL modeling. Funding for this work was provided by the United States Geological Survey under Contract Nos. 08HQGR0037 and G12AP20098. The contents of this paper reflect the views of the authors, who are responsible for the facts and accuracy of the data presented herein. The contents do not necessarily reflect the official views or policies of the United States federal government. This paper does not constitute a standard, specification, or regulation. This material is based on research performed in a renovated collaboratory by the National Science Foundation under Grant No. 0963183, which is an award funded under the American Recovery and Reinvestment Act of 2009 (ARRA).

References

Afacan, K.B. (2014). "Evaluation of Nonlinear Site Response of Soft Clay Using Centrifuge Models." Ph.D. thesis, Univ. of California, Los Angeles, CA.

Afacan, K.B., Brandenberg, S.J., and Stewart, J.P. (2014). "Centrifuge modeling studies of site response in soft clay over wide strain range." *J. Geotech. Geoenviron. Eng.,* 140(2), 04013003

Blake, T.F., Hollingsworth, R.A., and Stewart, J.P., editors (2002). "Recommended procedures for implementation of DMG Special Publication 117 Guidelines for analyzing and mitigating landslide hazards in California," Southern California Earthquake Center, University of Southern California, Los Angeles, California, 130 pgs.

Bolton, M. D. (1986). "The strength and dilatancy of sands." *Geotechnique* 36(1), 65-78.

Borcherdt, R.D. (1994). “Estimates of site-dependent response spectra for design (methodology and justification),” *Earthquake Spectra*, 10(4), 617-653.

Boulanger, R.W. and Idriss, I.M. (2007). “Evaluation of cyclic softening in silts and clays,” *J. Geotech. Geoenviron. Eng.*, 133(6), 641–652.

Brennan, A.J., Thusyanthan, N.I., Madabhushi, S.P.J., (2005) “Evaluation of shear modulus and damping in dynamic centrifuge tests.” *J. Geotech Geoenviron Eng. ASCE*, 131(12):1488–1497

Darendeli, M. B. (2001). “Development of a new family of normalized modulus reduction and material damping curves.” Ph.D. thesis, Univ. of Texas, Austin, TX.

Dobry R., Borcherdt R.D., Crouse C.B., Idriss I.M., Joyner W.B., Martin G.R., Power M.S., Rinne E.E., Seed R.B. (2000). “New site coefficients and site classification system used in recent building seismic code provisions (1994/1997 NEHRP and 1997 UBC).” *Earthquake Spectra*, 16, 41–68.

Duku, P.M., Stewart, J.P., Whang, D.H., and Venugopal, R. (2007). “Digitally controlled simple shear apparatus for dynamic soil testing,” *Geotech. Testing J.*, 30 (5), 368-377.

Elgamal, A., Yang, Z., Parra, E., and Ragheb (2003). "A modeling of cyclic mobility in saturated cohesionless soils." *Int. J. Plasticity,* 19, 883-905.

Garnier, J., Gaudin, C., Springman, S.M., Culligan, P.J., Goodings, D., Konig, D., Kutter, B., Phillips, R., Randolph, M.F., and Thorel, L. (2007). "Catalogue of scaling laws and similitude questions in geotechnical centrifuge modeling." *Int. J. Physical Modeling in Geotechnics.* 3, 09-23.

Groholski, D.R., Hashash, Y.M., Kim, B., Musgrove, M., Harmon, J., and Stewart, J.P. (2016). "Simplified model for small-strain nonlinearity and strength in 1D seismic site response analysis." *J. Geotech. Geoenviron. Eng.*, 142(9), 04016042.

Hashash, Y. M. A., Musgrove, M. I., Harmon, J. A., Groholski, D. R., Phillips, C. A., and Park, D., (2016). DEEPSOIL 6.1, User Manual.

Isenhower, W.M., and Stokoe, K.H. (1981). "Strain-rate dependent shear modulus of San Francisco Bay mud." *Int. Conf. on Recent Adv. In Geotech. Earthquqke Eng. And Soil Dyn.*, Volume II, 597-602, St. Louis.

Kaklamanos, J., Bradley, B.A., Thompson, E.M., and Baise, L.G. (2013). “Critical parameters affecting bias and variability in site response analyses using KiK-net downhole array data,” *Bull. Seism. Soc. Am.*, 103, 1733-1749

Kaklamanos, J., Baise, L.G., Thompson, E. M., and Dorfmann, L. (2015). “Comparison of 1D linear, equivalent-linear, and nonlinear site response models at six KiK-net validation sites,” *Soil Dyn. and Earthquake Eng.*, 69, 207-219.

Khosravi, M., Meehan, C.L., Cacciola, D.V., and Khosravi, A. (2013). “Effect of fast shearing on the residual shear strengths measured along pre-existing shear surfaces in Kaolinite,” *Geo-Congress 2013*: pp. 245-254. doi: 10.1061/9780784412787.025

Kim, B. and Hashash, Y.M.A. (2013). “Site response analysis using downhole array recordings during the March 2011 Tohoku-Oki Earthquake and the Effect of Long-Duration Ground Motions,” *Earthquake Spectra*, 29, S37-S54.

Kim, B., Hashash, Y.M.A., Stewart, J.P., Rathje, E.M., Harmon, J.A., Musgrove, M.I., Campbell, K.W., and Silva, W.J. (2016). “Relative differences between nonlinear and equivalent-linear 1D site response analyses,” *Earthquake Spectra*, 32, 1845-1865.

Kwok, A.O., Stewart, J.P., Hashash, Y.M.A., Matasovic, N., Pyke, R., Wang, Z.,and Yang, Z. (2007).“Use of exact solutions of wave propagation problems to guide implementation of nonlinear seismic ground response analysis procedures.” *J. Geotech. & Geoenv. Eng.*, 133 (11), 1385-1398.

Ladd, C.C. (1991). “Stability evaluation during staged construction,” *J. Geotech. Eng.*, 117(4), 540–615.

Lefebvre, G. and LeBoeuf, D. (1987). “Rate effects and cyclic loading of sensitive clays,” *J. Geotech. Engrg.,* 113(5), 476-489.

Mayne, P.W. and Kulhawy, F.H. (1982), “Ko -OCR relationships in soil,” *J. Geotech. Engrg. Div.*, 108(6), 851-872.

Matesic, L., and Vucetic, M. (2003). "Strain-rate effect on soil secant shear modulus at small cyclic strains." *J. Geotech. Geoenviron. Eng.* 126(6), 536-549.

Mazzoni, S., McKenna, F., Scott, M.H., Fenves, G.L., et. al., 2009. OpenSees, Command Language Manual

Meehan, C.L., Boulanger, R.W., and Duncan, J.M. (2008). “Dynamic centrifuge testing of slickensided shear surfaces,” *J. Geotech. Geoenviron. Eng.*, 134(8), 1086–1096.

Matasovic, N., and Hashash, Y. (2012). *Practices and Procedures for Site-Specific Evaluations of Earthquake Ground Motions, Synthesis 428,* National Cooperative Highway Research Program, Transportation Research Board, Washington D.C.

Phillips, C. and Hashash, Y.M.A. (2009). “Damping formulation for nonlinear 1D site response analyses,” *Soil Dyn. and Earthquake Eng.*, 29 (7), 1143–1158.

Phillips, C., Kottke, A.R., Hashash, Y.M.A., and Rathje, E.M. (2012). “Significance of ground motion time step in one dimensional site response analysis,” *Soil Dyn. and Earthquake Eng.*, 43, 202–217.

Qiu, T. (2010). “Analytical solution for Biot flow–induced damping in saturated soil during shear wave excitations.” *Journal of geotechnical and geoenvironmental engineering*, 136(11), 1501-1508.

Shafiee, A., Stewart, J.P., Venugopal, R. and Brandenberg, S.J. (2017). “Adaptation of bi-directional broadband simple shear device for constant volume and stress-controlled testing,” *Geotech. Testing J.*, 42(1), 15-28.

Sheahan, T.C., Ladd, C.C., and Germaine, J.T. (1996). ”Rate-dependent undrained shear behavior of saturated clay.” *J. Geotech. & Geoenviron. Eng.*, 122 (2), 99–108.

Stewart, J.P., Afshari, K, and Hashash, Y.M.A. (2014). “Guidelines for performing hazard-consistent one-dimensional ground response analysis for ground motion prediction,” *PEER Report 2014/16*, Pacific Earthquake Engineering Research Center, Berkeley, CA.

Stewart, J.P., Afshari, K., Goulet, C.A. (2017). Non-ergodic site response in seismic hazard analysis, *Earthquake Spectra*, 33(4), 1385-1414.

Yee, E., Stewart, J.P., and Tokimatsu, K. (2013). “Elastic and large-strain nonlinear seismic site response from analysis of vertical array recordings,” *J. Geotech. Geoenviron. Eng.*, 139 (10), 1789-1801.

Yong, R. N., and Japp, R.D. (1969). "Stress-strain behavior of clays in dynamic compression." Vibration effects of earthquakes on soils and foundations, *ASTM Special Technical Publication 450*, 233-262.

Yniesta, S., and Brandenberg, S.J. (2017). “Stress-Ratio-Based Interpretation of Modulus Reduction and Damping Curves.” *J. Geotech. Geoenvir. Eng.*, 143(1), 06016021.

Yniesta, S., Brandenberg, S.J. and Shafiee, A. (2017). “ARCS: A one dimensional nonlinear soil model for ground response analysis.” Soil Dynamics and Earthquake Engineering. 102, 75-85.

Zalachoris, G., and E. M. Rathje (2015). Evaluation of one-dimensional site response techniques using borehole arrays, *J. Geotech. Geoenviron. Eng.*, 141(12), 04015053.

Table 1. Configuration of six models analyzed in this study.

Model	NL or EL	Modeling Platform	Constitutive Model	Yee et al. (2013) Strength Correction[a]	Rate Correction
1	NL	DEEPSOIL	GQ/H[b]	No	1.00
2	NL	DEEPSOIL	GQ/H	Yes	1.00
3	NL	DEEPSOIL	GQ/H	Yes	1.82
4	NL	DEEPSOIL	ARCS[c]	Yes	1.82
5	NL	OpenSees	PIMY/PDMY[d]	Yes	1.82
6	EL	DEEPSOIL	NA	Yes	1.82

[a] The Yee et al. (2013) rate correction was applied to the Darendeli (2001) modulus reduction curve.

[b] Groholski et al. (2016)

[c] Yniesta et al. (2017)

[d] Elgamal et al. (2003)

Figure 1

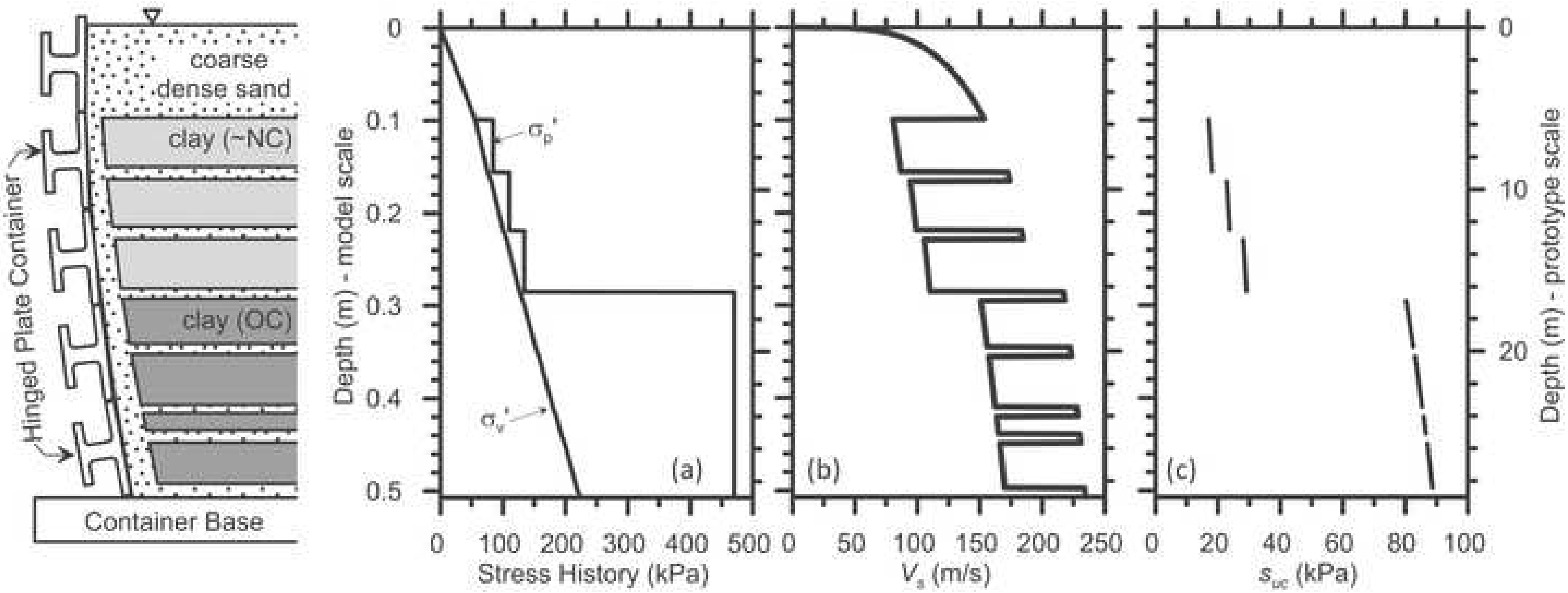
coarse
dense sand
clay (~NC)
clay (OC)
Hinged Plate Container
Container Base
Depth (m) - model scale
0
0.1
0.2
0.3
0.4
0.5
σp'
σv'
(a)
0
100
200
300
400
500
Stress History (kPa)
(b)
0
50
100
150
200
250
Vs (m/s)
(c)
0
20
40
60
80
100
suc (kPa)
Depth (m) - prototype scale
0
10
20

Figure 2

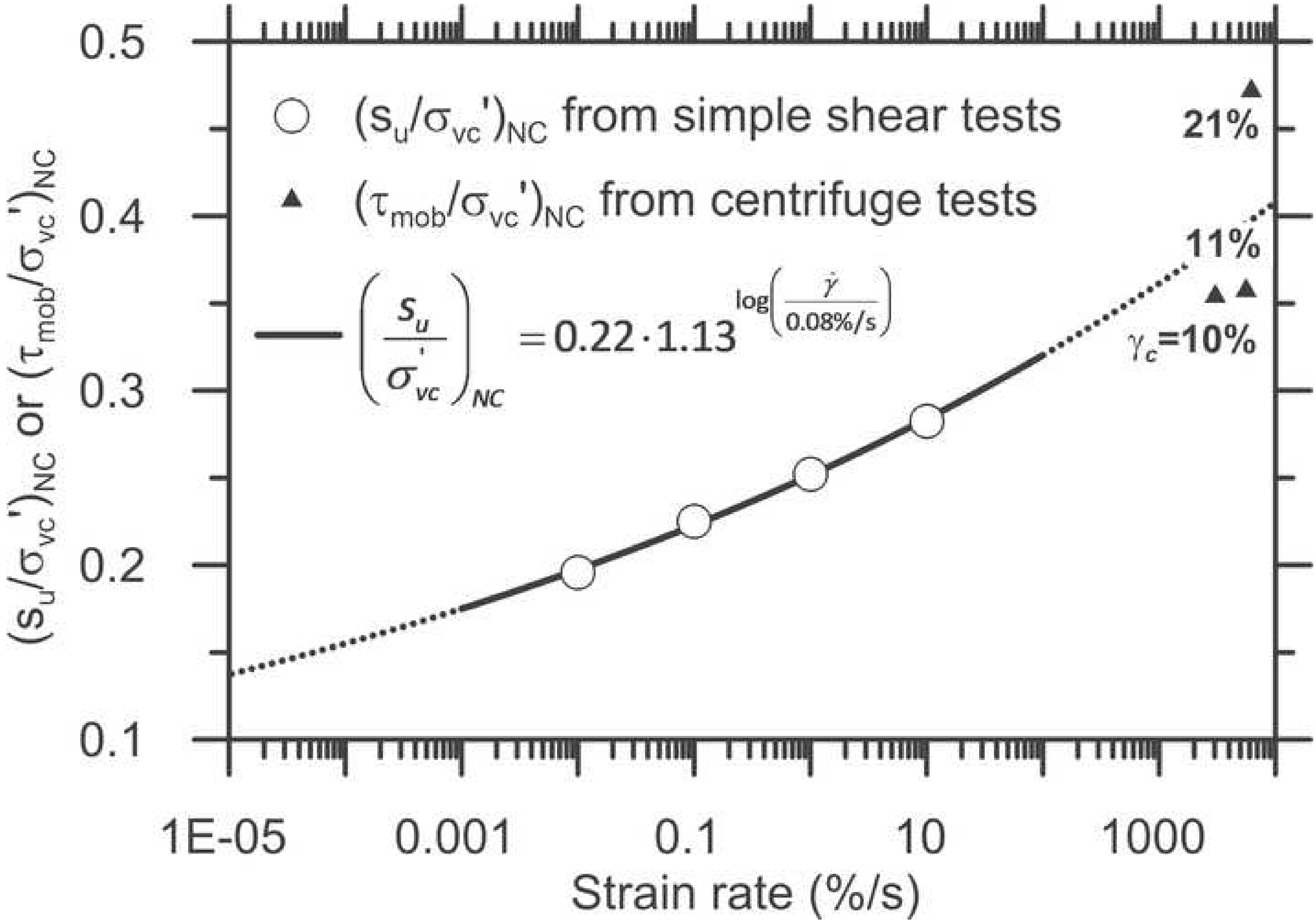

0.5
0.4
0.3
0.2
0.1
$(s_u/\sigma_{vc}')_{NC}$ or $(\tau_{mob}/\sigma_{vc}')_{NC}$
$(s_u/\sigma_{vc}')_{NC}$ from simple shear tests
$(\tau_{mob}/\sigma_{vc}')_{NC}$ from centrifuge tests
$\left(\frac{s_u}{\sigma_{vc}'}\right)_{NC} = 0.22 \cdot 1.13^{\log\left(\frac{\dot{\gamma}}{0.08\%/s}\right)}$
21%
11%
γ_c=10%
1E-05
0.001
0.1
10
1000
Strain rate (%/s)

Figure 3

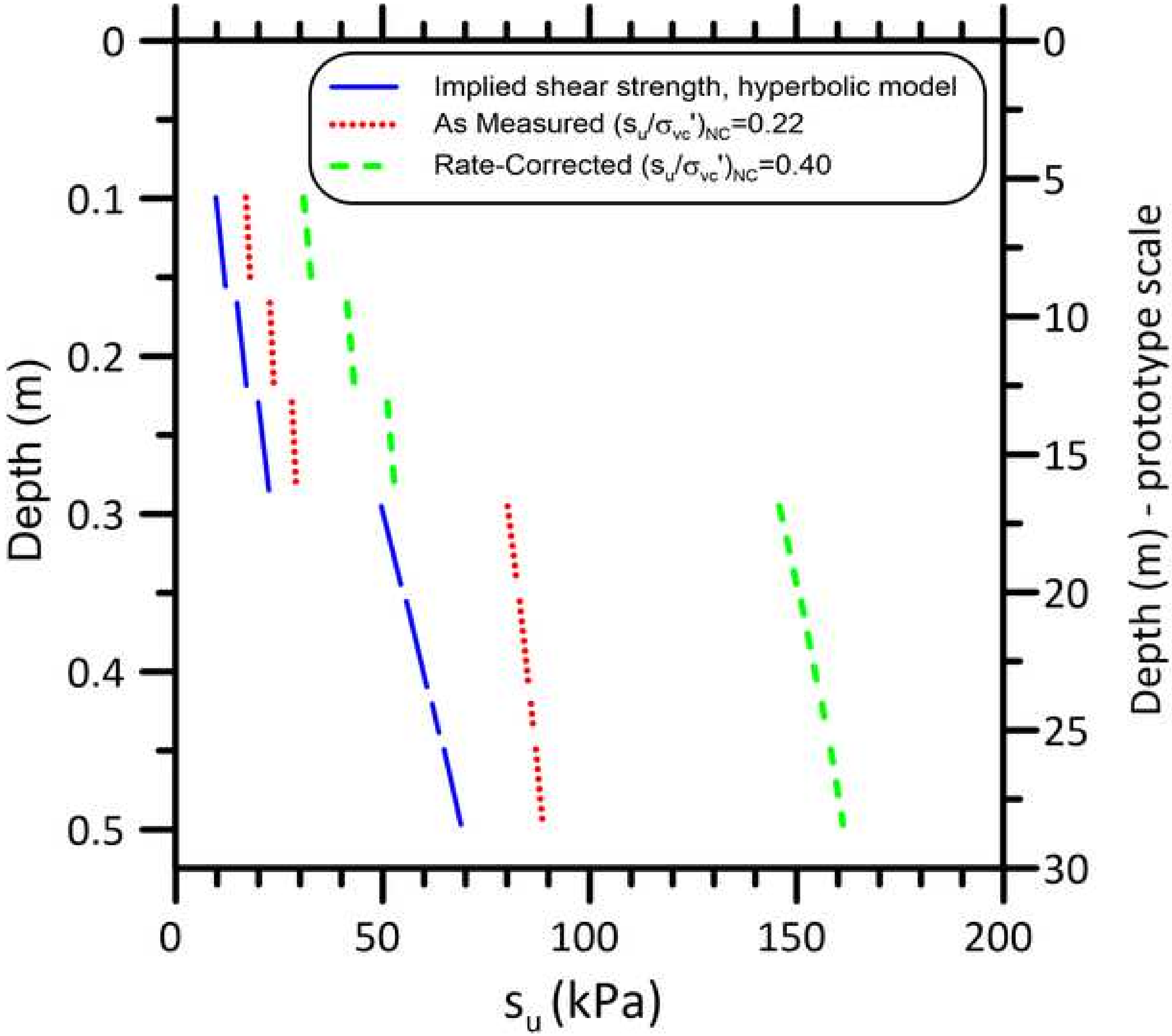

Implied shear strength, hyperbolic model
As Measured (s_u/σ_vc')_NC=0.22
Rate-Corrected (s_u/σ_vc')_NC=0.40
Depth (m)
0
0.1
0.2
0.3
0.4
0.5
Depth (m) - prototype scale
0
5
10
15
20
25
30
0
50
100
150
200
s_u (kPa)

Figure 4

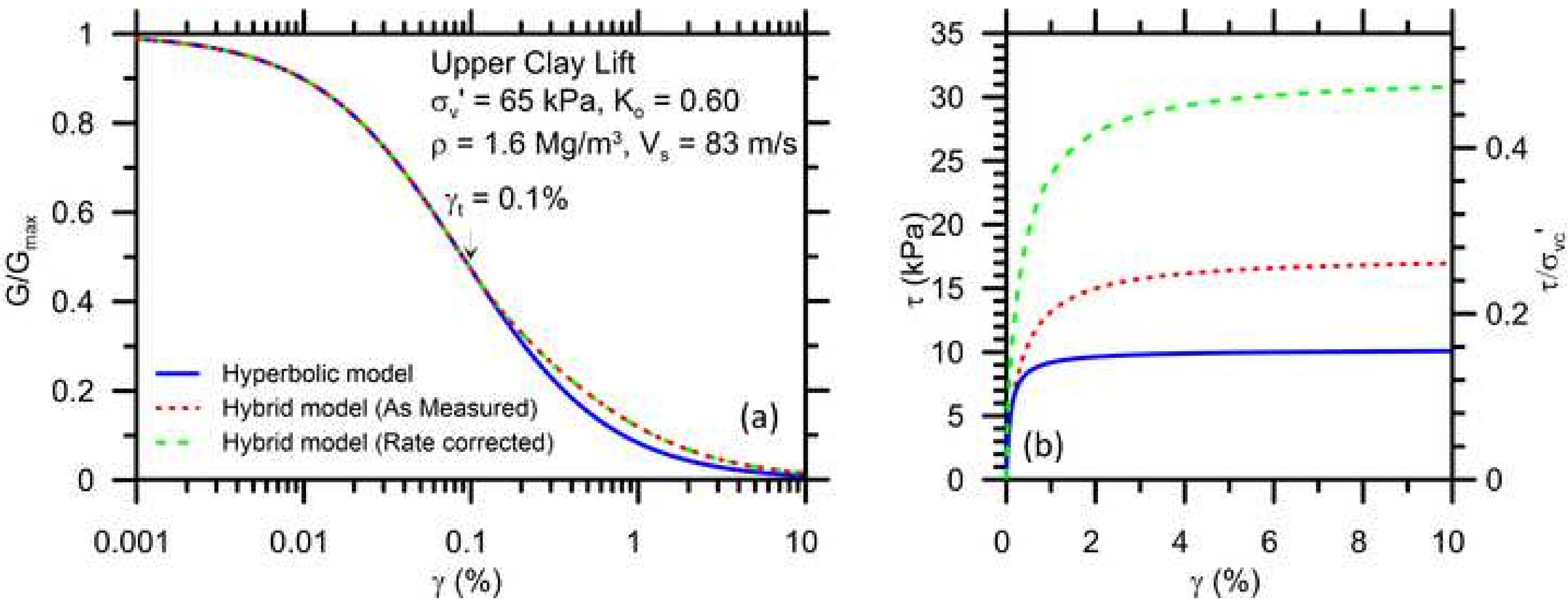
Upper Clay Lift
σv' = 65 kPa, Ko = 0.60
ρ = 1.6 Mg/m³, Vs = 83 m/s
γt = 0.1%
Hyperbolic model
Hybrid model (As Measured)
Hybrid model (Rate corrected)
(a)
G/Gmax
γ (%)
(b)
τ (kPa)
τ/σvc'
γ (%)

Figure 5

Click here to access/download;Figure;Fig5.tif

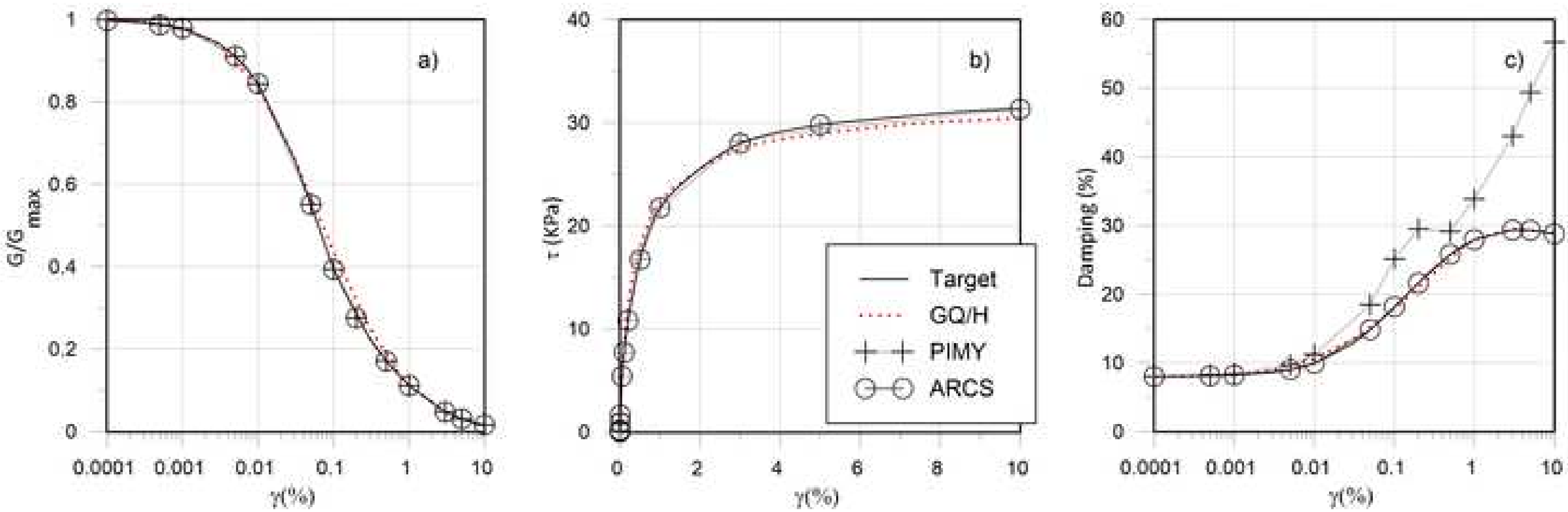

Figure 6

Click here to access/download;Figure;Fig6_ver2.tif

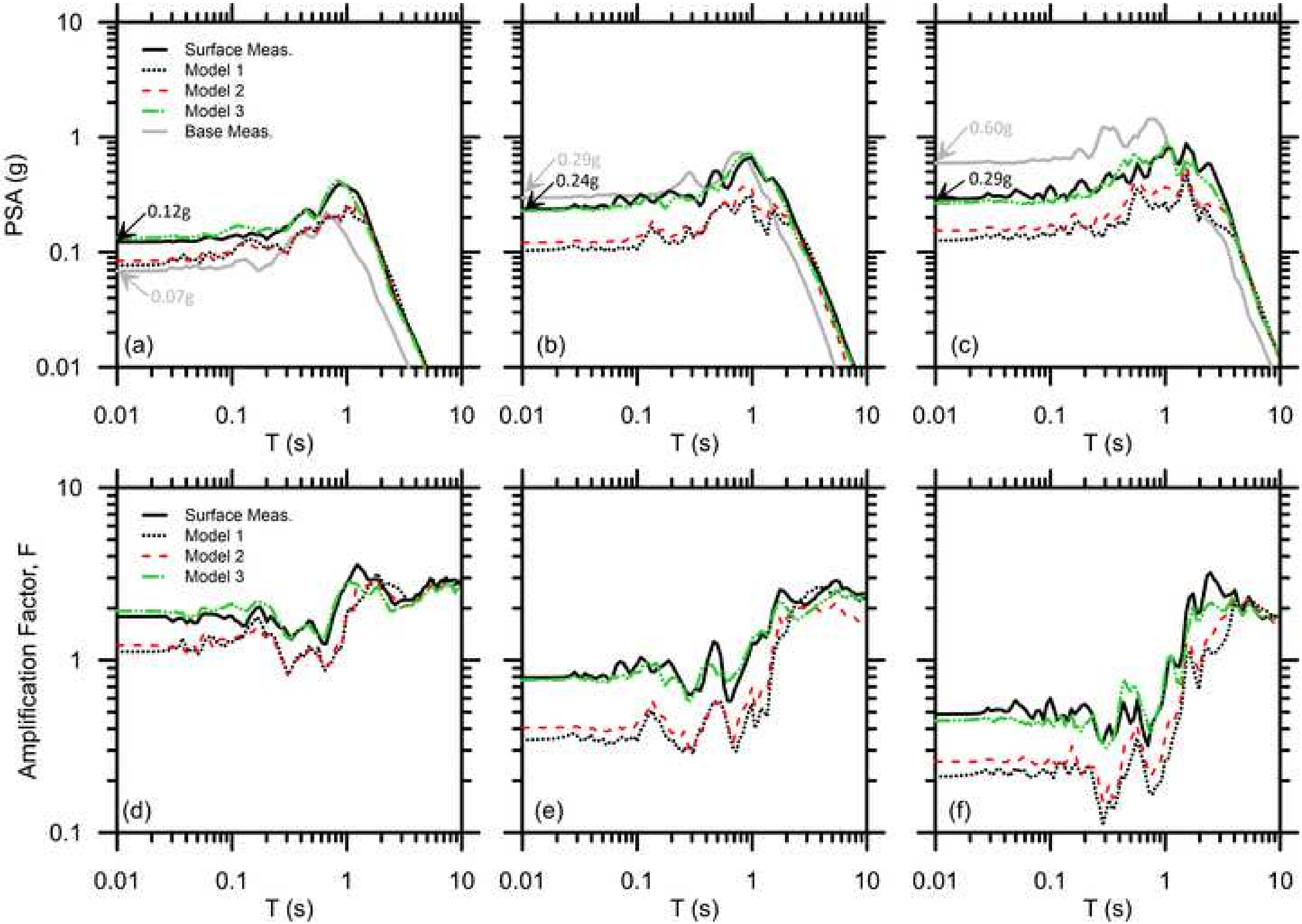

Figure 7

Click here to access/download;Figure;Fig7.tif

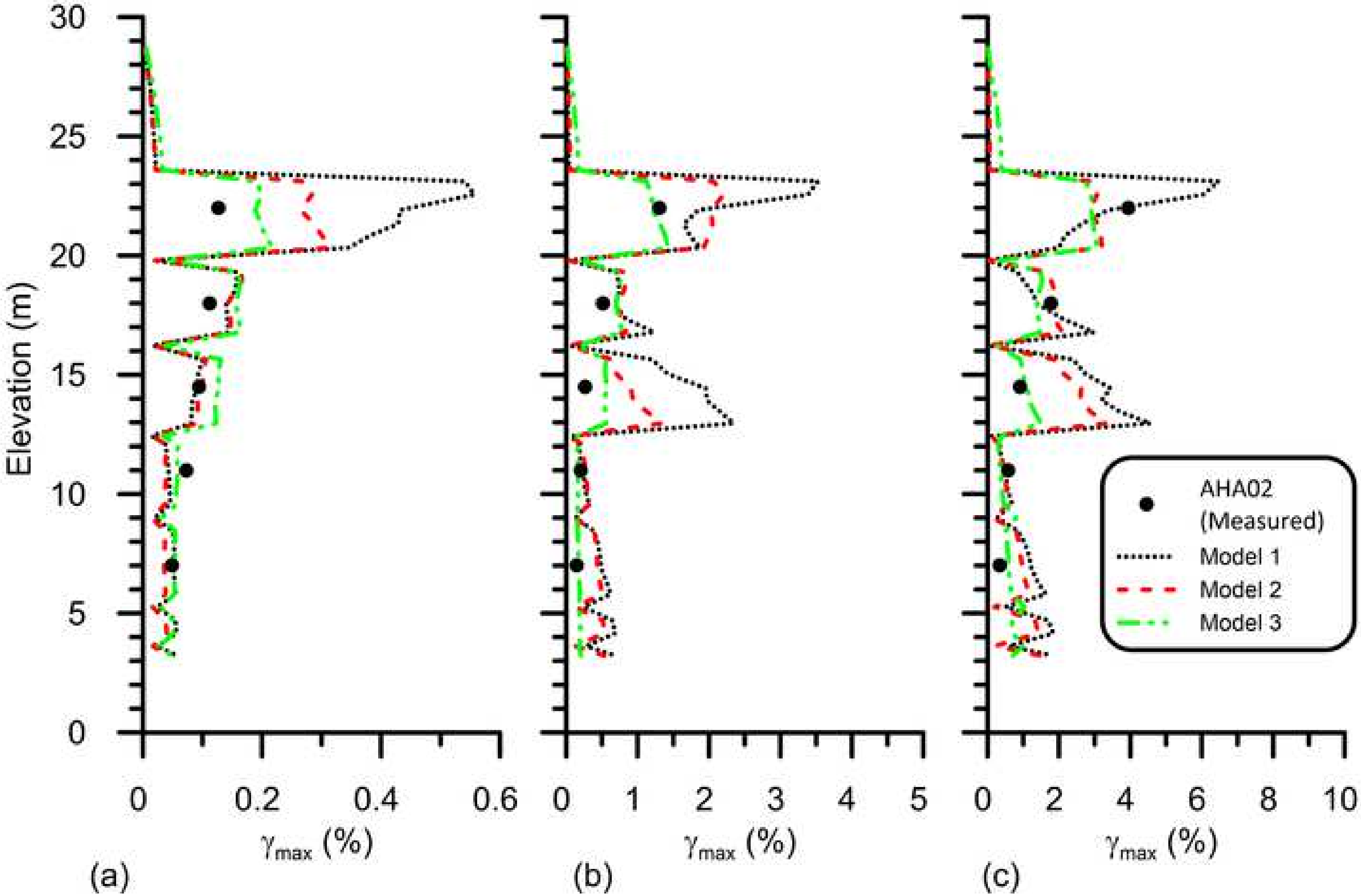

Figure 8

Click here to access/download;Figure;Fig8.tif

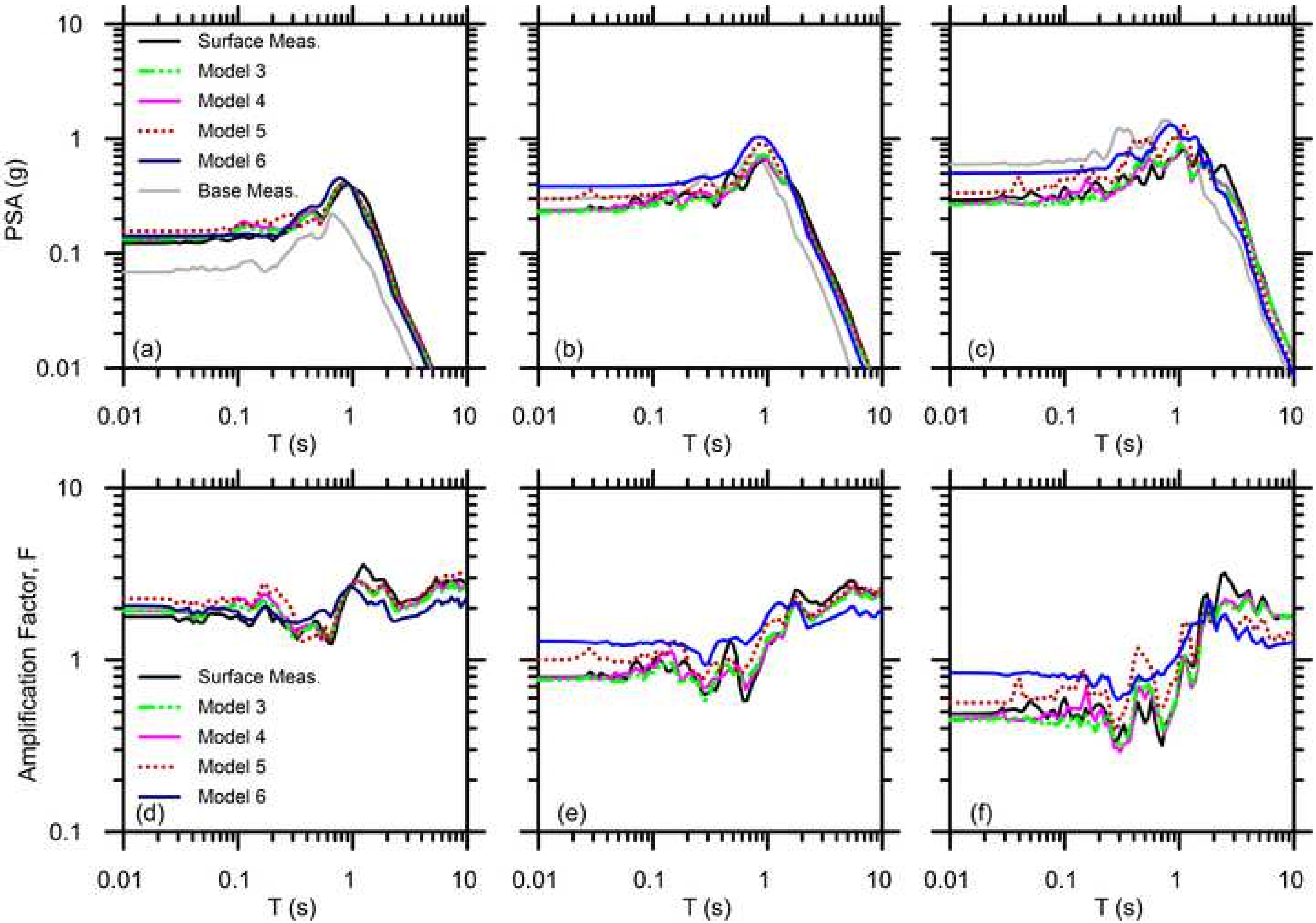

Figure 9

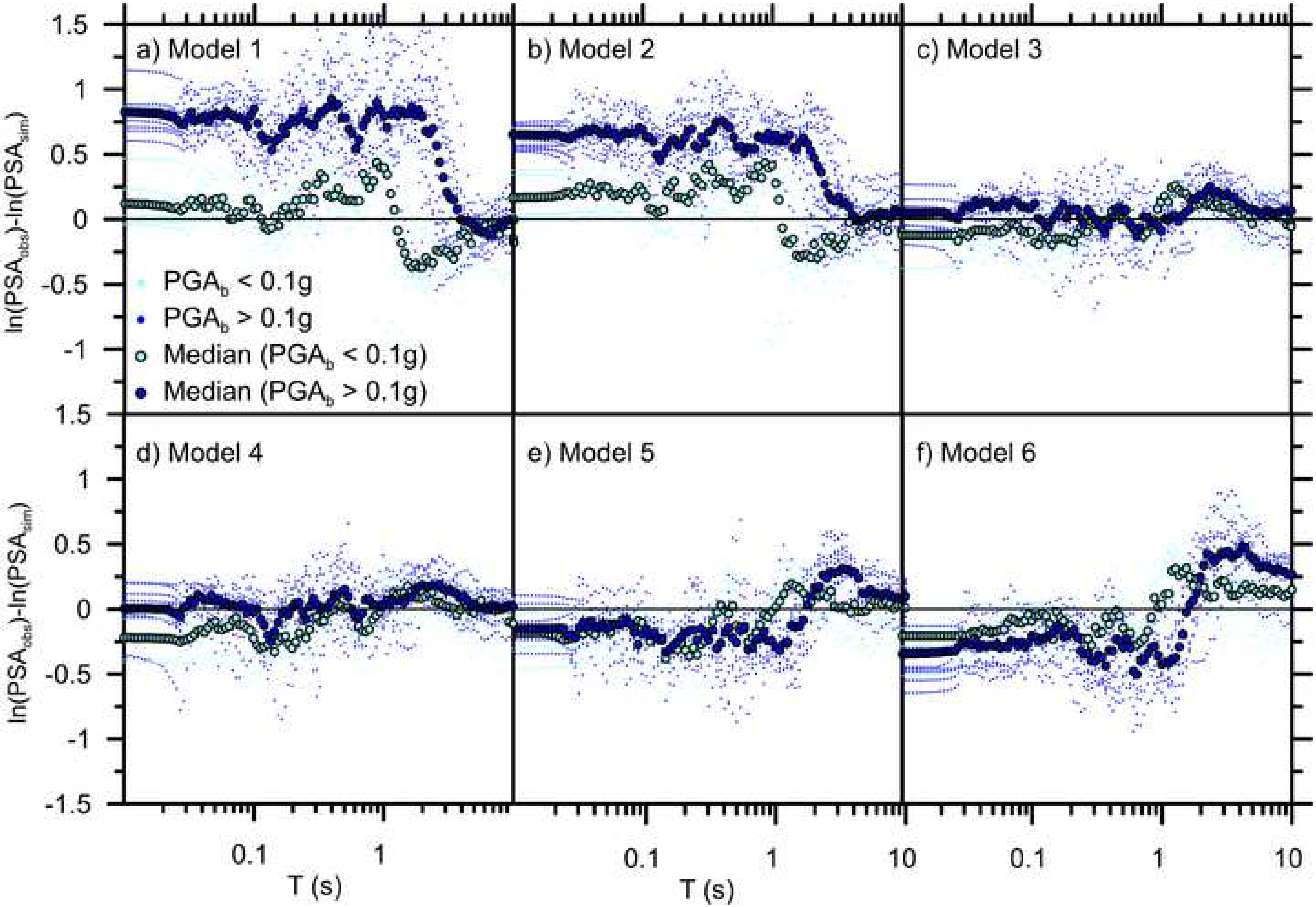
a) Model 1
b) Model 2
c) Model 3
d) Model 4
e) Model 5
f) Model 6
PGA_b < 0.1g
PGA_b > 0.1g
Median (PGA_b < 0.1g)
Median (PGA_b > 0.1g)
ln(PSA_obs)-ln(PSA_sim)
1.5
1
0.5
0
-0.5
-1
-1.5
0.1
1
10
T (s)

Figure 1. Properties of centrifuge model AHA02 showing (a) stress history, (b) shear wave velocity, and (c) monotonic undrained shear strength. Modified from Afacan et al. (2014)

Figure 2. Normally consolidated strength ratio of Bay Mud as a function of shear strain rate.

Figure 3. Profiles of implied, measured, and rate-adjusted shear strengths. Depth in prototype units.

Figure 4. Illustration of Yee et al. (2013) curve-fitting procedure to obtain a desired shear strength. The backbone curve is plotted with shear stress normalized by monotonic shear strength at a strain rate of 0.08%/s.

Figure 5. Modulus reduction (a), backbone (b) and damping ratio (c) curves predictions for the GQ/H (Groholski et al. 2016), Pressure Independent Multi Yield (Elgamal et al. 2003) and Axis Rotation Cubic Spline (ARCS) (Yniesta et al. 2017) models.

Figure 6. Pseudo-spectral accelerations (5% damping) and spectral amplification factors for (a and d) small, (b and e) medium, and (c and f) high intensity Rinaldi Receiving Station ground motion for Models 1, 2 and 3.

Figure 7. Profiles of measured and predicted peak shear strain for (a) small, (b) medium, and (c) high intensity Rinaldi Receiving Station ground motion for models 1, 2, and 3.

Figure 8. Measured and computed PSAs (5% damping) and amplification factors for (a and d) small, (b and e) medium, and (c and f) high intensity Northridge Rinaldi Receiving Station ground motion. Predictions for DEEPSOIL (Model 3), ARCS (Model 4) OpenSees (Model 5) and DEEPSOIL-EQL (Model 6).

Figure 9. PSA residuals vs oscillator period for weak and moderate/strong groups of input motions for the six simulation types from Table 1.